ELSEVIER

Physica A 267 (1999) 487–498

PHYSICA A

www.elsevier.com/locate/physa

Jamming transition in pedestrian counter flow

Masakuni Muramatsu, Tunemasa Irie, Takashi Nagatani*

Division of Thermal Science, College of Engineering, Shizuoka University, Hamamatsu 432-8561, Japan

Received 14 January 1999

Abstract

A lattice gas model with biased random walkers is presented to mimic the pedestrian counter flow in a channel under the open boundary condition of constant density. There are two types of walkers without the back step: the one is the random walker going to the right and the other is the random walker going to the left. It is found that a dynamical jamming transition from the freely moving state at low density to the stopped state at high density occurs at the critical density. The transition point is given by $p_c = 0.45 \pm 0.01$, not depending on the system size. The transition point depends on the strength of drift and decreases with increasing drift. Also, we present the extended model to take into account the traffic rule in which a pedestrian walks preferably on the right-hand side of the channel.

PACS: 05.70.Fh; 89.40.+k; 05.90.+m

Keywords: Pedestrian flow; Traffic flow; Phase transition

1. Introduction

Recently, traffic problems have attracted considerable attention [1,2]. The one-dimensional traffic flow problems have been studied by various traffic models: the cellular automaton models, the car following models, the gas kinetic models, and the hydrodynamic models [3–29]. The jamming transitions between the freely moving traffic and the jammed traffic have been found in their traffic models. The transition has been observed in the actual highway traffic [21]. The two-dimensioinal traffic flow is more complex than the one-dimensional case. The two-dimensional traffic has been investigated only by the cellular automaton models [30–33]. It has been found that the

* Corresponding author. Fax: +81-478-1048.
E-mail address: tmtnaga@eng.shizuoka.ac.jp (T. Nagatani)

0378-4371/99/$ - see front matter
PII: S0378-4371(99)00018-7

jamming transition similar to the one-dimensional traffic occurs in the two-dimensional case.

The pedestrian flow dynamics is closely related with the traffic flow dynamics. However, the studies of the pedestrian flow are scarce [34–36]. To know the properties of pedestrian flow is important in our life. Especially, it will be necessary to avoid the jammed state of pedestrians in the channel of the subway. The modeling and simulation method for the traffic flow can be applied to the pedestrian flow. The pedestrian flow has been studied by a few researches. Henderson has conjectured that pedestrian crowds behave similar to gases or fluids [34]. Helbing has proposed the active walker model to describe human trail formation [35]. He has showed that pedestrian dynamics exhibits various collective phenomena interpreted as self-organization effects due to nonlinear interactions among pedestrians. Fukui and Ishibashi have proposed the cellular automaton model describing the pedestrian flow [36].

The pedestrian flow is interesting from the points of view of nonequilibrium phase transitions. There is an open question whether or not the dynamical jamming transition occurs. Is the jamming transition different from that in the two-dimensional traffic flow?

In this paper, we propose the lattice gas model for the pedestrian flow where a gas particle represents a pedestrian. A gas particle performs a biased random walk to a preferential direction with no back step. We study the counterflow of pedestrians in a channel of subway under the open boundary condition. We carry out simulation for the pedestrian counterflow. We show that a jamming transition occurs at a critical density with increasing density. Also, we study the dependence of the jamming transition on the system size, the drift strength, the boundary density, and the traffic rule.

2. Model

We describe the lattice gas model for the pedestrian counterflow in the two-dimensional system. Our model is a modified version of the lattice gas model used in the DLA simulation. It is called multi-particle DLA simulation. The model is defined on the square lattice of $W \times L$ sites where W is the width of the channel and L the length of the channel.

The pedestrian flow model is given by the lattice gas model with two components of particles. One component particle represents the walker going to the right and the other component particle represents the walker going to the left. Each particle moves to the preferential direction with no back step: the one-component particle moves to the right, up, or down and the other component particle moves to the left, up, or down. The particles perform the biased random walk. Each site contains only a single particle. The walker is inhibited from overlapping on the site. The excluded-volume effect is taken into account. Fig. 1 shows all the possible configurations of the right walker (going to the right). The cross point indicates the site occupied by the other (right or left) particles. The transition probabilities $p_{t,x}, p_{t,y}, p_{t,-y}$ of the right walker corresponding to each configuration are given by the following: $p_{t,x} = D + (1-D)/3$, $p_{t,y} = (1-D)/3$,

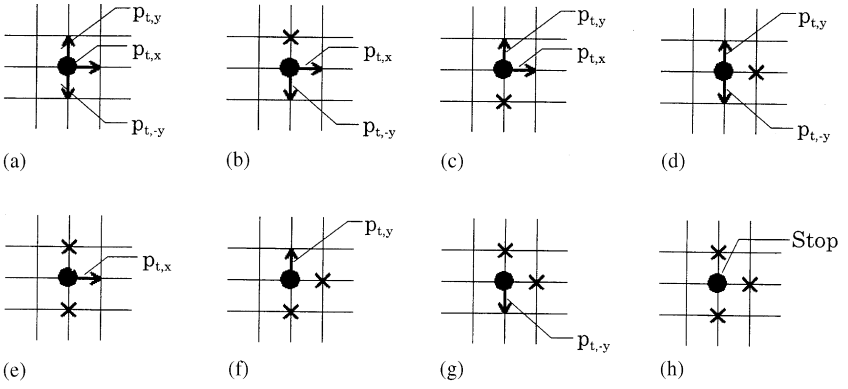

Fig. 1. All the possible configurations of the right walker (going to the right) on the square lattice. The full circle indicates the right walker. The cross point indicates the site occupied by the other walkers. The walker can move only to the unoccupied sites. The transition probabilities to the nearest-neighbor sites (to the right, up, and down) are given, respectively, by $p_{t,x}$, $p_{t,y}$, and $p_{t,-y}$.

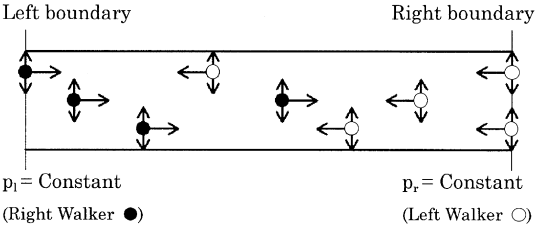

Fig. 2. Schematic illustration of the pedestrian counterflow in a channel. The channel is composed of the top and bottom walls. The right walker going to the right and the left walker going to the left are indicated by the full circle and the open circle. The left and right boundaries are open. The density of the left walker on the right boundary and the density of the right walker on the left boundary remain constant.

$p_{t,-y} = (1-D)/3$ for configuration (a), $p_{t,x} = D + (1-D)/2$, $p_{t,-y} = (1-D)/2$ for configuration (b), $p_{t,x} = D + (1-D)/2$, $p_{t,y} = (1-D)/2$ for configuration (c), $p_{t,y} = 1/2$, $p_{t,-y} = 1/2$ for configuration (d), $p_{t,x} = 1$ for configuration (e), $p_{t,y} = 1$ for configuration (f), $p_{t,-y} = 1$ for configuration (g), and $p_{t,x} = p_{t,y} = p_{t,-y} = 0$ for configuration (h), where D indicates the strength of the drift. Similarly, the transition probabilities $p_{t,-x}, p_{t,y}, p_{t,-y}$ of the left walker (going to the left) are given by replacing $p_{t,x}$ with $p_{t,-x}$.

Fig. 2 shows the schematic illustration of the pedestrian counterflow in a channel. The right walker going to the right is indicated by the full circle and the left walker going to the left is indicated by the open circle. The channel is composed of the top and bottom walls where the wall length is L and the interval between two walls is W. When the walker arrives at the wall, it is reflected by the wall and never go out through the wall. The left and right boundaries are open. The density p_l of the right walker on the left boundary is set by a constant value. The density p_r of the left walker on the right boundary is also set by a constant value. When the

right (left) walker arrives at the right (left) boundary, its walker is removed from the channel.

On the unit time step, all the walkers within the channel are updated only once: the update procedure is the random sequential update rule.

In this model, the pedestrian problem is reduced to its simplest form. The essential features are maintained. These features include the simultaneous flow of right and left walkers in two parallel directions in which walkers cannot overlap on a single site. It is expected that the jamming transition occurs due to the excluded-volume effect of the interaction between the right and left walkers.

3. Simulation and result

We describe the simulation procedure for our model. We carry out the computer simulation. Initially, there are no walkers within the channel. The right walkers are distributed randomly on the left boundary at probability p_l. The left walkers are also distributed randomly on the right boundary at probability p_r. All the walkers are numbered randomly from 1 to N where N is the number of walkers existing within the channel, including the walkers on the boundaries. Following the rule in Fig. 1, the numbered walkers are in order updated. After all the walkers are updated, if the walkers arrive at the boundaries, their walkers are removed from the channel. After the above procedure was carried out, one time step is completed. In the next time step, new right and left walkers are added on the left and right boundaries as the walker densities on both boundaries remain to be p_l and p_r. The above procedure is repeated.

We present the simulation result obtained by the above procedure. We define the total entrance density p as $p \equiv p_r + p_l$. The mean velocity $\langle v \rangle$ of walkers moving in a unit time interval is defined to be the value of the number of moving walkers divided by the total number of walkers existing in the channel. Fig. 3(a) shows the plot of the mean velocity $\langle v \rangle$ against the entrance density p in the case of the drift $D = 0.0$ for the width $W = 10, 20, 50, 100$, and 200 where the length L is 500. The mean velocity decreases slowly with increasing p. When the entrance density p is larger than the critical value, the mean velocity becomes zero. Fig. 3(b) shows the plot of the occupancy ρ against the total entrance density p where the simulation result in Fig. 3(b) is the same as that in Fig. 3(a). The occupancy is defined as the fraction of sites occupied by the walkers. The dotted line indicates $\rho = p$. The occupancy is slightly lower than the dotted line. The value of occupancy at the critical density $p_c = 0.45 \pm 0.01$ is given by $\rho_c = 0.38 \pm 0.01$.

Fig. 4 shows the typical patterns (a) and (b) obtained at time $t = 10\,000$ for densities $p = 0.20$ and $p = 0.50$ where $W = 50$, $L = 500$, and $D = 0.0$. The black and gray dots indicate, respectively, the right and left walkers. The pattern (a) represents the freely moving phase in which most walkers are able to move. The pattern (b) represents the perfectly stopped phase in which all walkers are not able to move.

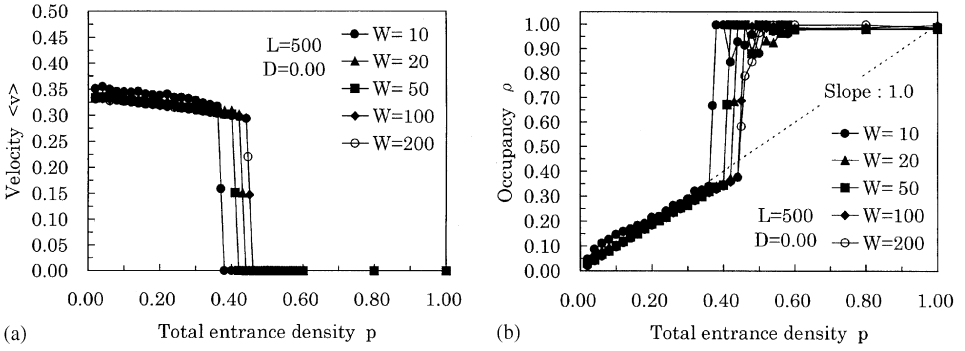

Fig. 3. (a) The plot of the mean velocity $\langle v\rangle$ against the total entrance density $p\,(=p_r+p_l)$ for $W=10$, 20, 50, 100, and 200 in the case of $D=0.0$ where $L=500$, and $t=10\,000$. (b) The plot of the occupancy ρ against the total entrance density p for the same data as (a).

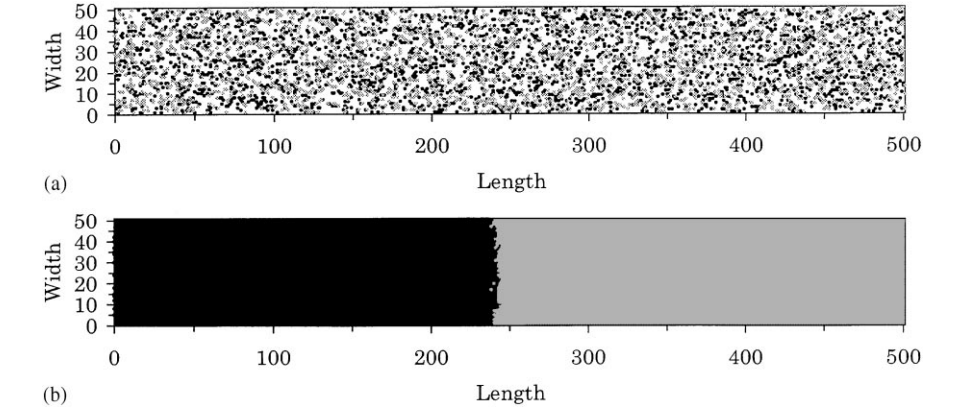

Fig. 4. The pedestrian patterns (a) and (b) obtained at $t=10\,000$ where $W=50$, $L=500$, and $D=0.0$. The black and gray dots represent, respectively, the right and left walkers. (a) The freely moving phase obtained at $p=0.20$. (b) The perfectly stopped phase obtained at $p=0.50$.

Fig. 5(a) and (b) show the plot of the mean velocity $\langle v\rangle$ and the plot of the occupancy against p for the drift $D=0.40$. The transition point is given by $p_c=0.31\pm0.01$. The critical density is lower than that of $D=0.0$. Fig. 6 shows the plots of the critical density p_c against the inverse $1/W$ of the width for $D=0.0$ and 0.40. When the width W is larger than 100, the critical density p_c reaches to the constant $p_c=0.45\pm0.01$ for $D=0.0$ and $p_c=0.31\pm0.01$ for $D=0.4$. It is found that the jamming transition does not depend on the system size. The jamming transition will be the first-order phase transition. Fig. 7 shows the time evolution of the flow out rate and the mean velocity where $W=50$, $L=500$, $D=0.0$, and $p=0.50$. Near $t=2000$, the flow out rate reaches the maximum value. The mean velocity $\langle v\rangle$ decreases to zero near $t=3500$. We study the dependence of the mean velocity $\langle v\rangle$ and the occupancy ρ on the drift D where $W=100$, $L=500$, and $t=10\,000$. Fig. 8 shows (a) the plot of the mean velocity $\langle v\rangle$ against the total entrance density p for $D=0.0, 0.10, 0.40, 0.70$ and (b) the plot of the

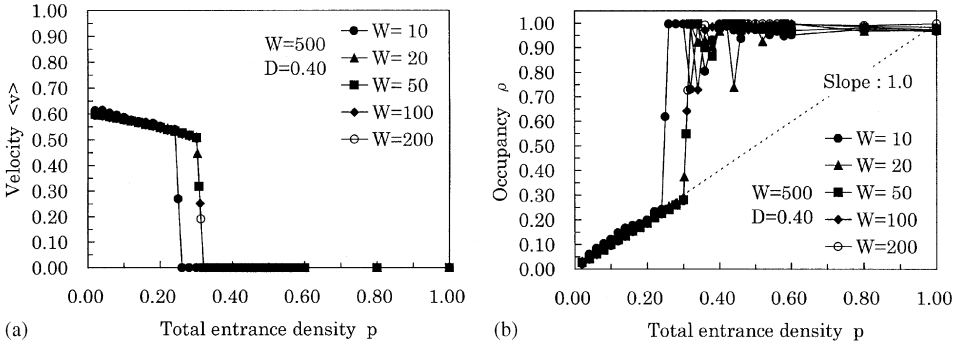

Fig. 5. (a) The plot of the mean velocity $\langle v\rangle$ against the total entrance density $p\,(=p_r+p_l)$ for $W=10$, 20, 50, 100, and 200 in the case of $D=0.4$ where $L=500$, and $t=10\,000$. (b) The plot of the occupancy ρ against the total entrance density p for the same data as (a).

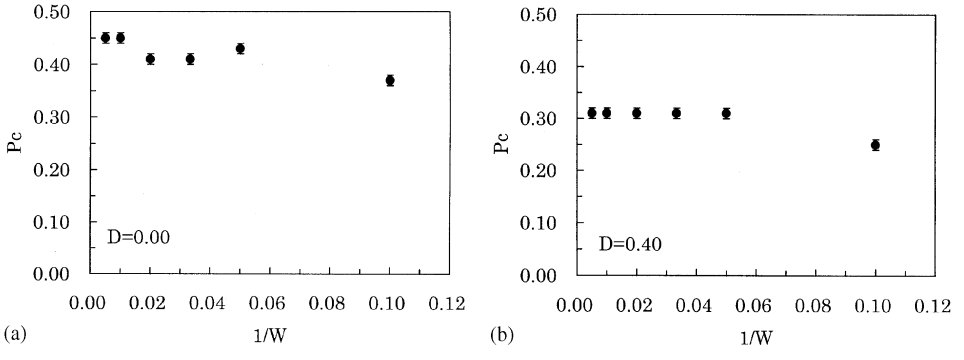

Fig. 6. The plots of the critical density p_c against the inverse $1/W$ of the width for $D=0.0$ and 0.4.

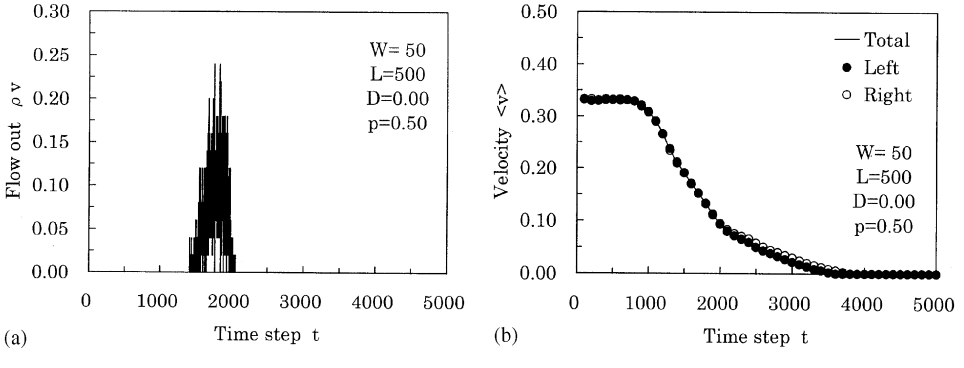

Fig. 7. (a) The plot of the quantity flowing out from both boundaries against time t in the perfectly stopped phase where $W=50$, $L=500$, $D=0.0$, and $p=0.50$. (b) The plot of the average velocity $\langle v\rangle$ against time t.

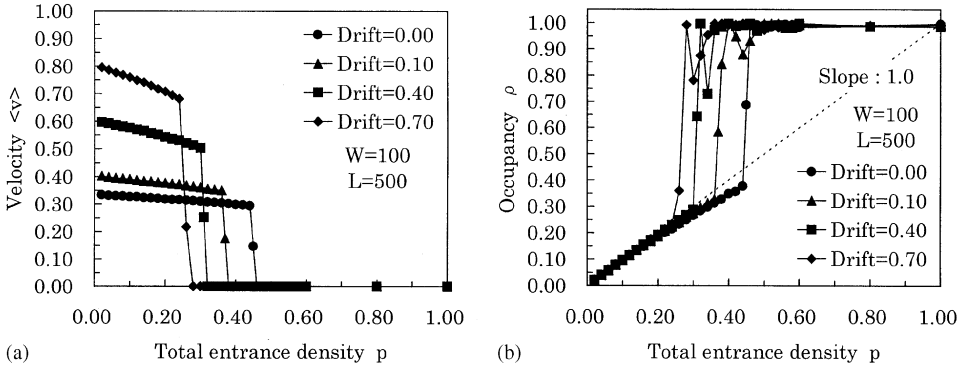

Fig. 8. The dependence of the mean velocity $\langle v \rangle$ and the occupancy ρ on the drift D where $W = 100$, $L = 500$, and $t = 10\,000$. (a) The plot of the mean velocity $\langle v \rangle$ against the total entrance density p for $D = 0.0$, 0.10, 0.40, and 0.70. (b) The plot of the occupancy ρ against the total entrance density p for the same data as (a).

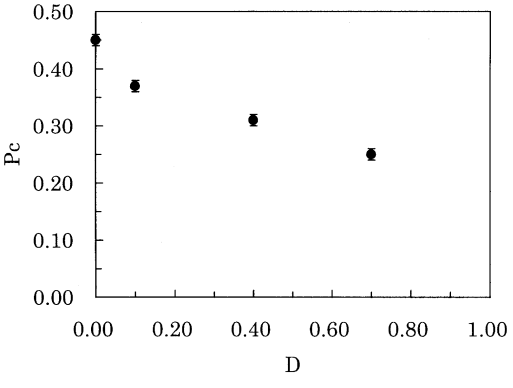

Fig. 9. The plot of the critical density p_c against the drift D where $W = 100$ and $L = 500$.

occupancy ρ against the total entrance density p for the same data as (a). The mean velocity increases with increasing drift. The critical density decreases with increasing drift. Fig. 9 shows the plot of the critical density p_c against the drift D where $W = 100$ and $L = 500$. The critical density p_c decreases with increasing drift.

We study the dependence of the mean velocity and the occupancy on the fraction c. The fraction c is defined as the ratio of the right walkers to all the walkers on the boundaries. Fig. 10 shows the plots of the mean velocity $\langle v \rangle$ and the occupancy ρ against the total entrance density p for the fraction $c = 1/2, 1/3$, and $1/5$, where $p_r = cp$, $p_l = (1-c)p$, $W = 100$, $L = 500$, $D = 0.4$, and $t = 10\,000$. The mean velocity and the occupancy do not depend on the fraction c. The jamming transition does not also depend on the fraction c.

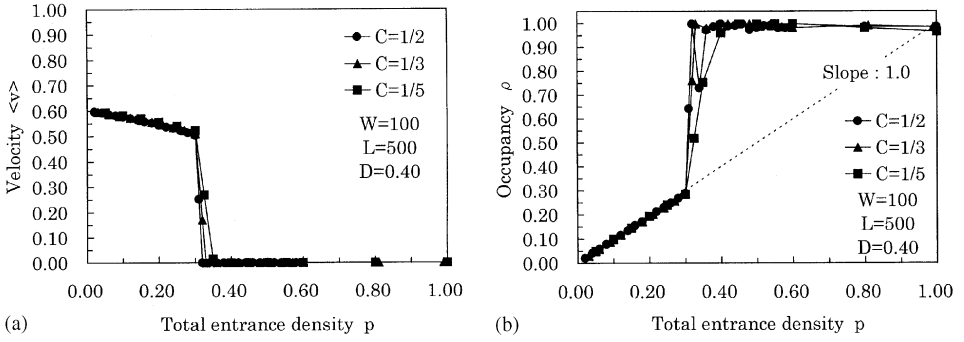

Fig. 10. The dependence of the mean velocity $\langle v\rangle$ and the occupancy ρ on the fraction c where $p_r = cp$, $p_l = (1-c)p$, $W = 100$, $L = 500$, $D = 0.4$, and $t = 10\,000$. (a) The plot of the average velocity $\langle v\rangle$ against the total entrance density p for $c = 1/2, 1/3$, and $1/5$. (b) The plot of the occupancy ρ against the total entrance density p for the same data as (a).

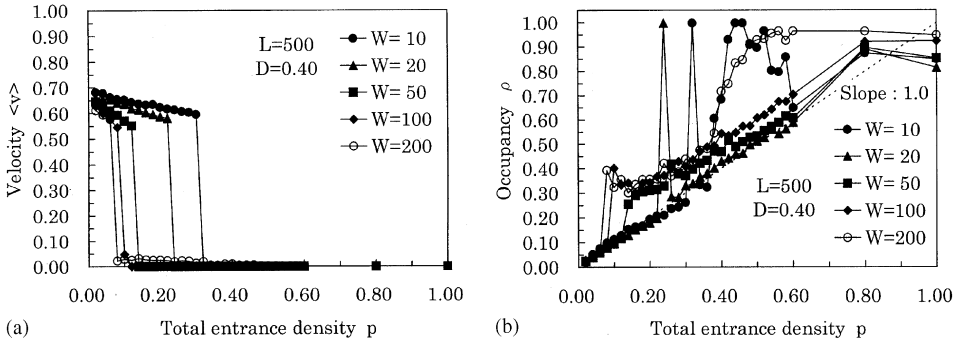

Fig. 11. The dependence of the mean velocity and the occupancy on the traffic rule of the right priority where $p_{t,-y} = 2p_{t,y}$ for the right walker. (a) The plot of the mean velocity $\langle v\rangle$ against the total entrance density $p\ (=p_r + p_l)$ for $W = 10, 20, 50, 100$, and 200 in the case of $D = 0.4$ where $L = 500$, and $t = 10\,000$. (b) The plot of the occupancy ρ against the total entrance density p for the same data as (a).

4. The extended model

We extend the above model to take into account the traffic rule. The pedestrian is obligated to walk on the right-hand side of the channel or road in Japan. The walker has the priority to move on the right-hand side of the channel. Therefore, we introduce the following traffic rule for the transition probabilities of the walker: the walker moves preferably to the right direction in the configurations (a) and (d) of Fig. 1, i.e. $p_{t,-y} > p_{t,y}$ for the right walker. The extended model except for $p_{t,-y} > p_{t,y}$ is the same as the model in Section 2. The simulation procedure including the update rule is the same as Section 3. We carry out the simulation for $p_{t,-y} = 2p_{t,y}$.

We study the dependence of the mean velocity $\langle v\rangle$ and the occupancy ρ on the traffic rule of the right priority where $p_{t,-y} = 2p_{t,y}$ for the right walker. Fig. 11(a) shows the plot of the mean velocity $\langle v\rangle$ against the total entrance density $p\ (=p_r + p_l)$ for $W = 10, 20, 50, 100$, and 200 in the case of $D = 0.4$ where $L = 500$, and $t = 10\,000$.

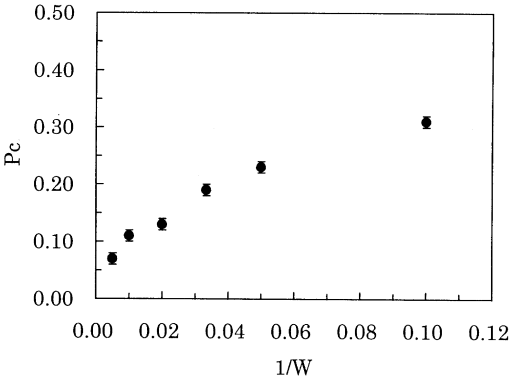

Fig. 12. The plot of the critical density p_c against the inverse $1/W$ of the width for the extended model taking into account the traffic rule of the right priority where $L = 500$ and $D = 0.4$.

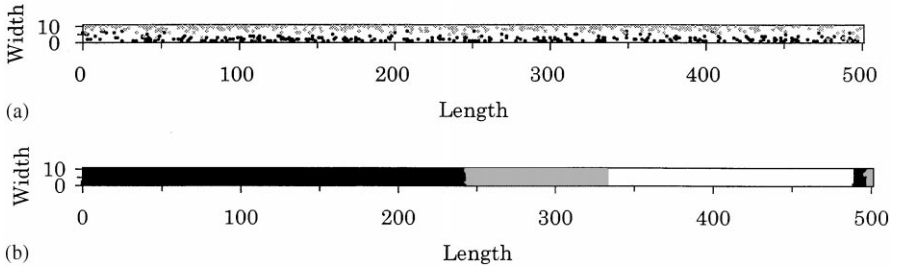

Fig. 13. The typical pedestrian patterns obtained for $W = 10$ where $L = 500$, $D = 0.4$, and $t = 10\,000$. The black and gray dots represent, respectively, the right and left walkers. (a) The freely moving phase at $p = 0.10$. (b) The almost stopped phase at $p = 0.40$.

Fig. 11(b) shows the plot of the occupancy ρ against the total entrance density p for the same data as (a). The mean velocity decreases sharply to a very small value at the critical density. The critical density decreases upon increasing the width W of the channel. The occupancy increases sharply near the transition point but the increment is less than that for no priority. This is due to the formation of empty regions in which no walkers exist.

We study the dependence of the critical density p_c on the width W. Fig. 12 shows the plot of the critical density p_c against the inverse $1/W$ of the width where $L = 500$ and $D = 0.4$. With increasing W, the critical density decreases. In the limit of $W \to \infty$, the critical density approaches a very small value or zero.

We study the pedestrian patterns in the freely moving phase and in the almost or perfectly stopped phase. Fig. 13 shows the typical pedestrian patterns obtained for $W = 10$ where $L = 500$, $D = 0.4$, and $t = 10\,000$. The black and gray dots represent, respectively, the right and left walkers. The pattern (a) exhibits the freely moving phase at $p = 0.10$. The pattern (b) exhibits the almost stopped phase at $p = 0.40$. Fig. 14 shows the typical pedestrian patterns obtained for $W = 50$ where $L = 500$, $D = 0.4$,

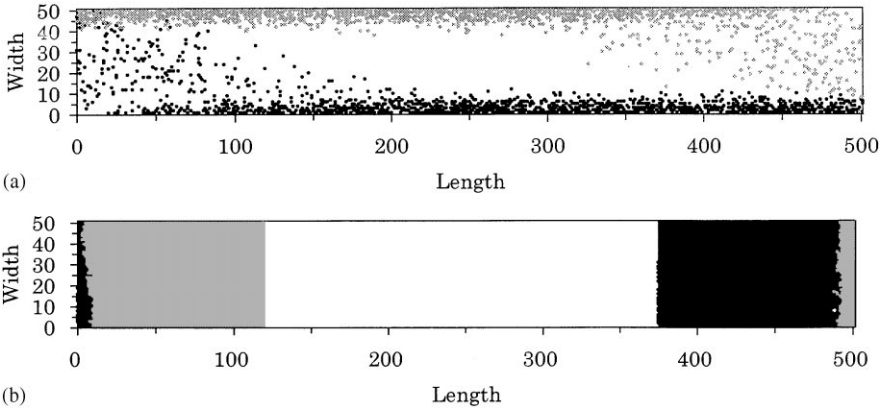

Fig. 14. The typical pedestrian patterns obtained for $W = 50$ where $L = 500$, $D = 0.4$, and $t = 10\,000$. The black and gray dots represent, respectively, the right and left walkers. (a) The freely moving phase at $p = 0.10$. (b) The almost stopped phase at $p = 0.40$.

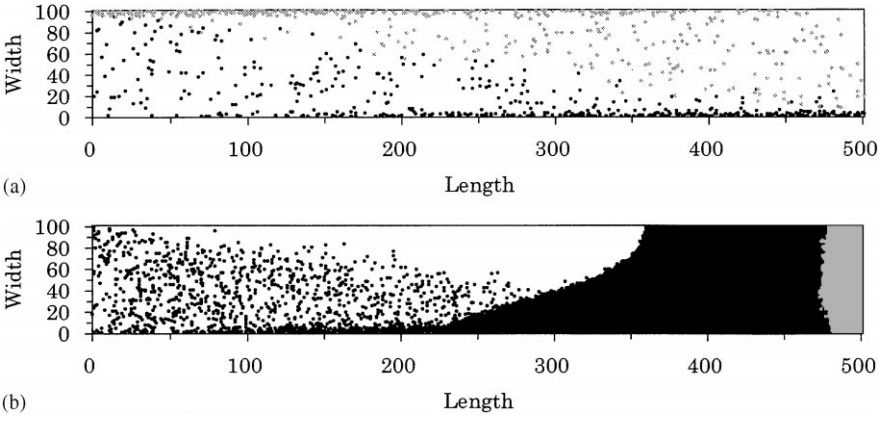

Fig. 15. The typical pedestrian patterns obtained for $W = 100$ where $L = 500$, $D = 0.4$ and $t = 10\,000$. The black and gray dots represent, respectively, the right and left walkers. (a) The freely moving phase at $p = 0.02$. (b) The perfectly stopped phase at $p = 0.10$.

and $t = 10\,000$. The patterns (a) and (b) exhibit the freely moving phase at $p = 0.10$ and the almost stopped phase at $p = 0.40$. Fig. 15 shows the typical pedestrian patterns obtained for $W = 100$ where $L = 500$, $D = 0.4$, and $t = 10\,000$. The patterns (a) and (b) exhibit the freely moving phase at $p = 0.02$ and the perfectly stopped phase at $p = 0.10$. In the freely moving phase at low density, the right walkers move near the bottom wall and the left walkers move near the top wall. The right walkers segregate from the left walkers. In the most stopped phase at high density, the right walkers and left walkers pile up against each other and the stripped structure is formed. There are no walkers in the empty regions indicated by the white color. Only the walkers on the edges move up or down. Almost all walkers excluding the walkers on the edges

cannot move and stop. With increasing width, it takes a longer distance for the right walkers to segregate with the left walkers. Under the constant length L, with increasing width W, the segregation is hard to occur. The decrease of the critical density with increasing width will be due to the segregation. It is found that the traffic rule has an important effect on the jamming transition in the pedestrian counterflow.

5. Summary

We presented the lattice gas model to mimic the pedestrian flow. We investigated the counter flow in a channel under the open boundary condition of constant density. We found that a dynamical jamming transition between the freely moving phase and the stopped phase occurs at a critical density. We studied the dependence of the jamming transition on the system size, the drift strength, and the traffic rule. We showed that the jamming transition does not depend on the system size but is highly dependent on the drift and the traffic rule.

It will be useful to investigate the various pedestrian flows with the use of the lattice gas model proposed here.

References

[1] D.E. Wolf, M. Schreckenberg, A. Bachem (Eds.), Traffic and Granular Flow, World Scientific, Singapore, 1996.
[2] D. Helbing, Verkehrsdynamik, Springer, Berlin, 1997.
[3] G.F. Newell, Oper. Res. 9 (1961) 209.
[4] G.B. Whitham, Proc. Roy. Soc. London A 428 (1990) 49.
[5] M. Bando, K. Hasebe, A. Nakayama, A. Shibata, Y. Sugiyama, Phys. Rev. E 51 (1995) 1035.
[6] K. Nagel, M. Schreckenberg, J. Physique I 2 (1992) 2221.
[7] M. Schreckenberg, A. Schadschneider, K. Nagel, N. Ito, Phys. Rev. E 51 (1995) 2329.
[8] G. Csanyi, J. Kertestz, J. Phys. A 28 (1995) 427.
[9] S.C. Benjamin, N.F. Johnson, P.M. Hui, J. Phys. A 29 (1996) 3119.
[10] A. Schadschneider, M. Schreckenberg, Ann. Phys. 6 (1997) 541.
[11] E. Ben-Naim, P.L. Krapivsky, S. Redner, Phys. Rev. E 50 (1994) 822.
[12] T. Nagatani, Phys. Rev. E 51 (1995) 922.
[13] I. Prigogine, R. Herman, Kinetic Theory of Vehicular Traffic, Elsevier, New York, 1971.
[14] S.L. Paveri-Fontana, Transportation Res. 9 (1975) 225.
[15] D. Helbing, Phys. Rev. E 53 (1996) 2366.
[16] D. Helbing, Physica A 233 (1996) 253.
[17] T. Nagatani, Physica A 237 (1997) 67.
[18] B.S. Kerner, P. Konhauser, Phys. Rev. E 48 (1993) 2335.
[19] B.S. Kerner, P. Konhauser, M. Schilke, Phys. Rev. E 51 (1995) 6243.
[20] S. Krauss, P. Wagner, C. Gawron, Phys. Rev. E 55 (1997) 5597.
[21] B.S. Kerner, H. Rehborn, Phys. Rev. E 53 (1996) R1297.
[22] D.A. Kurtze, D.C. Hong, Phys. Rev. E 52 (1995) 218.
[23] T. Komatsu, S. Sasa, Phys. Rev. E 52 (1995) 5574.
[24] T. Nagatani, K. Nakanishi, Phys. Rev. E 57 (1998) 6415.
[25] T. Nagatani, K. Nakanishi, H. Emmerich, J. Phys. A 31 (1998) 5431.
[26] T. Nagatani, Phys. Rev. E 58 (1998) 4271.
[27] T. Nagatani, Physica A 202 (1994) 449.

[28] A. Awazu, J. Phys. Soc. Japan 67 (1998) 1071.
[29] K. Nagel, D.E. Wolf, P. Wagner, P. Simon, Phys. Rev. E 58 (1998) 1425.
[30] O. Biham, A.A. Middelton, D.A. Levine, Phys. Rev. A 46 (1992) R6124.
[31] T. Nagatani, Phys. Rev. E 48 (1993) 3290.
[32] J.A. Cuesta, F.C. Matinez, J.M. Nolera, A. Sanchez, Phys. Rev. E 48 (1993) 4175.
[33] K.H. Chung, P.M. Hui, G.Q. Gu, Phys. Rev. E 51 (1995) 772.
[34] L.F. Henderson, Nature 229 (1971) 381.
[35] D. Helbing, Phys. Rev. E 51 (1995) 4282.
[36] M. Fukui, Y. Ishibashi, Proc. 5th Symp. on Simulation of Traffic flow, 1998 (in Japanese).